Water Adsorption on Rh(111) at 20 K: From Monomer to Bulk Amorphous Ice

Susumu Yamamoto, Atsushi Beniya, Kozo Mukai, Yoshiyuki Yamashita, and Jun Yoshinobu*

The Institute for Solid State Physics, The University of Tokyo, 5-1-5 Kashiwanoha, Kashiwa, Chiba 277-8581, Japan

Received: December 9, 2004; In Final Form: January 28, 2005

The adsorption of water (D_2O) molecules on Rh(111) at 20 K was investigated using infrared reflection absorption spectroscopy (IRAS). At the initial stage of adsorption, water molecules exist as monomers on Rh(111). With increasing water coverage, monomers aggregate into dimers, larger clusters ($n = 3-6$), and two-dimensional (2D) islands. Further exposure of water molecules leads to the formation of three-dimensional (3D) water islands and finally to a bulk amorphous ice layer. Upon heating, the monomer and dimer species thermally migrate on the surface and aggregate to form larger clusters and 2D islands. Based on the temperature dependence of OD stretching peaks, we succeeded in distinguishing water molecules inside 2D islands from those at the edge of 2D islands. From the comparison with the previous vibrational spectra of water clusters on other metal surfaces, we conclude that the number of water molecules at the edge of 2D islands is comparable with that of water molecules inside 2D islands on the Rh(111) surface at 20 K. This indicates that the surface migration of water molecules on Rh(111) is hindered as compared with the cases on Pt(111) and Ni(111) and thus the size of 2D islands on Rh(111) is relatively small.

1. Introduction

Water is one of the most abundant and essential molecules in nature. This makes the interaction of water with metal surfaces important in various fields of science and technology such as corrosion, electrochemistry, and heterogeneous catalysis. The structure and properties of the first water layer on metal surfaces have been intensively investigated to understand the water−metal interface for decades.[1,2] Nonetheless, there remain many open questions about the atomic level structure of the water−metal interface and controversy still exists. This is mainly because water molecules show complex behaviors depending on the metal substrate and experimental conditions including coverage and temperature.

Water molecules on metal surfaces form various low-dimensional structures, ranging from isolated monomers and small clusters, to one-dimensional (1D) chains, and two-dimensional (2D) islands and ordered overlayers.[1,2] As the water coverage increases, water molecules form a hydrogen-bonding (H-bonding) network and grow into three-dimensional (3D) islands and ultimately into bulk ice.[1,2]

These structures and their stabilities are determined by the interplay between (i) water−water and (ii) water−substrate interactions. On most metal surfaces, the intermolecular hydrogen bonds between water molecules (water−water interactions) are comparable in strength to those formed between the molecule and the substrate (water−substrate interactions). Moreover, the subtle energy balance between water−water and water−substrate interactions depends on the underlying substrate. From a thermodynamic point of view, this energy balance can be divided into three levels: (1) water−water interactions are stronger than water−substrate interactions (water molecules do not wet the surface and form 3D islands); (2) water−substrate interactions are stronger than water−water interactions (water molecules wet the surface and sometimes form the 2D epitaxial layer that is in registry with the substrate lattice); and (3) water−substrate interactions are much stronger than water−water interactions (a water molecule is dissociated on the surface).

Among all the adsorbed structures of water molecules on metal surfaces, the ordered 2D overlayers have been investigated most intensively as a model structure at the water−metal interface. The structure of the first water layer on metal surfaces has long been considered to be an ice-like bilayer where water molecules arrange in buckled hexagonal rings as in ice Ih. In the "bilayer" model, proposed by Doering and Madey,[3] the O atoms lie in two planes separated by 0.96 Å; only half of the molecules are directly bonded to a metal surface via an oxygen lone pair orbital. Both H atoms belonging to a lower lying water form hydrogen bonds with neighboring water molecules. A higher lying water contributes one H to the hexagonal H-bonding network and another free OH bond is oriented along the surface normal. This model, in which the free OH is dangling into vacuum, is referred to as the "H-up" bilayer. This ordered overlayer often shows a $(\sqrt{3} \times \sqrt{3})R\,30°$ pattern in low-energy electron diffraction (LEED).[3,4] However, the detailed LEED study of water on Ru(001) by Held and Menzel[5] revealed that each plane of O atoms was not separated by 0.96 Å but by only 0.1 Å. A combined X-ray and computational study by Ogasawara et al.[6] also contradicted the "bilayer" model[3] and proposed that the first layer was nearly flat on Pt(111) when the multilayer was annealed at 140 K. They also proposed that the orientation of free OH bonds in the higher lying waters was toward the metal substrate ("H-down" bilayer). Recent density functional theory (DFT) calculations proposed that the vertically compressed bilayer model on Ru(001)[5] could be explained by a half-dissociated water layer.[7,8] However, a recent study of D_2O on Ru(001) using sum frequency generation (SFG) vibrational spectroscopy reported that the adsorbed D_2O molecules remained intact.[9] They also proposed the bilayer structure where

* Corresponding author. Fax: 81-4-7136-3474. E-mail: yoshinobu@issp.u-tokyo.ac.jp.

10.1021/jp044379d CCC: $30.25
Published on Web 03/08/2005

every second water molecule exhibited a hydrogen−metal substrate bond ("H-down" bilayer).

Besides the controversy in the bilayer, other low-dimensional structures of water molecules on metal surfaces such as monomers and clusters remain poorly understood. While the "bilayer" ice is in a thermodynamically stable state because it is usually prepared on metal surfaces at high temperatures (just below the desorption temperature), water clusters are in a thermodynamically metastable state. These metastable clusters can be observed only at low temperatures and at low coverages. At low temperatures, the surface diffusion of water molecules is suppressed. Thus, on low-temperature metal surfaces it is likely for adsorbed water molecules to form metastable clusters and not to form 2D islands until the coverage is sufficiently high.

In recent years, scanning tunneling microscopy (STM) has been used to study submonolayer water molecules on the (111) surfaces of Au,[10] Ag,[11−13] Cu,[14,15] Pt,[16,17] and Pd.[18] At low coverages, cyclic hexamers were observed on Ag(111),[11−13] Cu(111),[14] and Pd(111)[18] surfaces. Furthermore, various size clusters smaller than hexamers, ranging from monomers to pentamers, were observed on the Pd(111) surface.[18] Despite its atomic resolution capability, it has not been possible with STM to resolve the internal structure of adsorbed H_2O molecules or to determine the orientation of H_2O molecules with respect to the surface normal ("H-up" or "H-down"). However, using DFT calculation and STM simulation, Cerdá et al. interpreted the STM images of water submonolayers on Pd(111) and proposed the novel structure where most water molecules were flat-lying and arranged in planar hexagons.[19]

Cluster formation at submonolayer coverages has been reported by several groups using vibrational spectroscopies such as high-resolution electron energy loss spectroscopy (HREELS),[20−22] infrared reflection absorption spectroscopy (IRAS),[23−28] and helium atom scattering (HAS).[29] On both Cu(100) and Pd(100) surfaces, water monomers can be isolated at 10 K, but warming to 20 K results in surface diffusion and clustering.[20] In addition, water monomers were identified on Al(111) at 20 K.[21] On the Pt(111) surface, Ogasawara et al. reported that monomers and dimers coexisted at 25 K; heating the surface to 40 K resulted in the dissociation of dimers into monomers as well as aggregation into clusters and bilayer ice.[24] In contrast, Nakamura et al. proposed that only dimers were present on Pt(111) at 20 K; upon heating to 40 K, dimers did not break up into monomers but formed tetramers.[25] In addition, Glebov et al. proposed that water adsorbed as monomers on Pt(111) at 23 K; at temperatures above 40 K, water molecules clustered into dimers and trimers.[29] On Ru(001)[26,27] and Ni(111)[28] surfaces, Nakamura and Ito reported the existence of water monomers at 20 K.

Despite these experimental findings on water clusters, our understanding of how the interplay between water−water and water−substrate interactions influences the behavior of metastable water clusters on metal surfaces is still limited. Here, we select Rh(111) as the underlying substrate for water adsorption for the following reasons. First, the interaction between the Rh(111) surface and water molecules is relatively strong as seen from the high desorption temperature of 190 K in temperature-programmed desorption (TPD) spectra.[30,31] Second, the Rh(111) surface has a lattice constant of 4.66 Å, which provides a closer match with bulk Ih ice, 4.52 Å,[32] than 4.68 Å for Ru(001). Note that water molecules on Rh(111) form an ordered structure with a $(\sqrt{3} \times \sqrt{3})R$ 30° diffraction pattern.[33] However, only a few investigations have reported on the interactions of water molecules with Rh(111).[30,31,33] In particular, the clustering behavior of water molecules on Rh(111) at low temperatures has not been reported yet.

In this study, we investigated the clustering behavior and ice formation of water molecules on Rh(111) at a low temperature of 20 K using IRAS. The present work aims to gain a general understanding of how the interplay between water−water and water−substrate interactions influences the clustering behavior of water molecules on metal surfaces, by comparing our results on Rh(111) with previous results on other metal surfaces.

2. Experimental Section

The experiments were performed in an ultrahigh vacuum chamber with a base pressure of $\sim 1 \times 10^{-8}$ Pa. The Rh(111) single-crystal substrate was cleaned by Ne ion sputtering, annealing, and flashing cycles. The orderliness was confirmed by LEED and the cleanness was checked by the adsorption behavior of CO using vibrational spectroscopy.[34] The substrate was cooled to 20 K by a cryogenic refrigerator. The temperature was monitored by a chromel−alumel (K-type) thermocouple spot-welded to the side of the crystal.

IRAS measurements were performed using an FTIR spectrometer (Bruker IFS66v/S) and a B-doped Si (Si:B) detector (the measurable range: 370−4000 cm^{-1}). All the spectra were taken at the sample temperature of 20 K with 4 cm^{-1} resolution and 500−1000 scans.

Water (D_2O) vapor was introduced onto the sample surface at 20 K through a pulse gas dosing system. The exposure was precisely controlled by the pulse duration, the number of shots, and the pressure in the gas line. The isotopic water, $D_2{}^{16}O$ (Aldrich, isotopic purity 99.96%), was degassed through several freeze−pump−thaw cycles before the deposition. The purity was also checked using a quadrupole mass spectrometer (QMS, Balzers QMS 200). In the present study, we used D_2O for the following reasons. First, the Si:B detector has much better sensitivity in the OD stretching region of D_2O than in the OH stretching region of H_2O. The second reason is to eliminate any influence of H_2O, which may adsorb from the background gas in the UHV chamber.

In this paper, the coverage of water molecules is described in terms of bilayer (BL), assuming that water molecules are arranged in buckled hexagonal rings as in ice Ih (see the Introduction). The "bilayer" structure shows a $(\sqrt{3} \times \sqrt{3})R$ 30° LEED pattern; two water molecules are contained in each unit cell. Thus, the saturation coverage of ideal bilayer ice is two-thirds of surface atoms on Rh(111); the atomic density on Rh(111) is given in terms of monolayer (ML) (1 ML = 1.61×10^{15} molecules/cm^2). Consequently, the absolute coverage of 1 BL is 1.07×10^{15} molecules/cm^2.

Coverage measurements were performed using TPD; the water coverage was determined by comparing each integrated area of the thermal desorption peak with that of 1 BL ice. The 1 BL ice was defined as the water ice layer which was prepared on Rh(111) by depositing water molecules onto the Rh surface held at 160 K until continuous dosing at this temperature led to the saturation in IRAS and TPD spectra.[33]

In TPD measurements, desorbing molecules were detected by a QMS with the ionization volume enclosed in a home-built small glass envelope ("Feulner cup"[35,36]). The single-crystal surface was placed in front of a small-sized (3.4-mm diameter) opening of this cup at a distance of 2 mm in TPD measurements. The advantage of this setup is an excellent signal-to-background ratio since the QMS ionization source only detects the desorbing molecules from the sample surface.

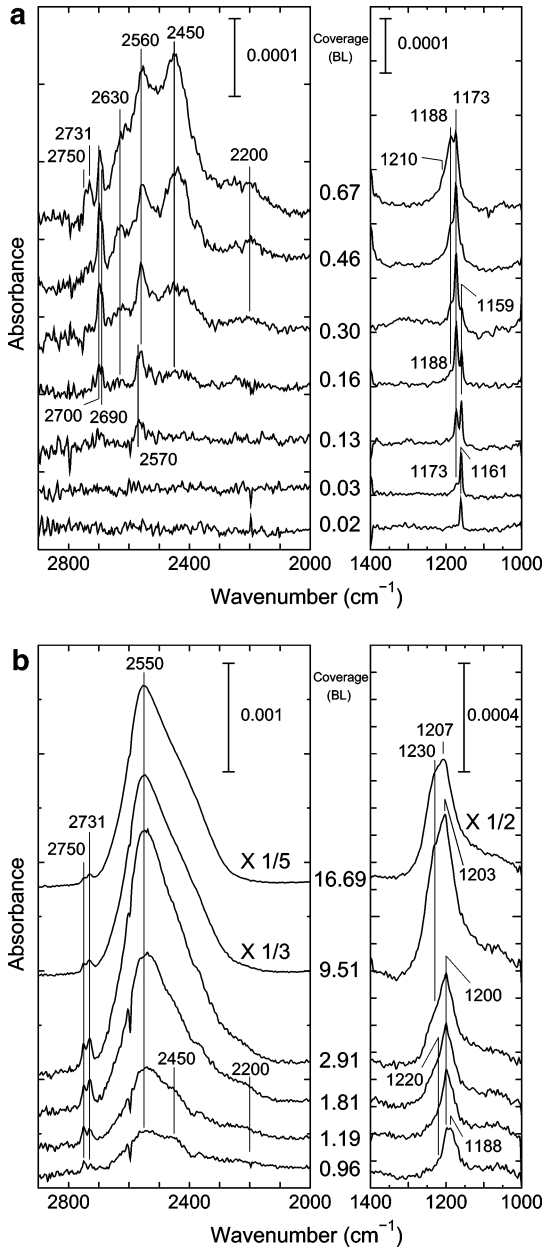

Figure 1. (a) IRAS spectra of D_2O on Rh(111) adsorbed at 20 K as a function of coverage (the low coverage region from 0.02 to 0.67 BL). All the spectra were measured at 20 K with 4 cm^{-1} resolution and 1000 scans. Each spectrum presented here is the average of five individual spectra. (b) IRAS spectra of D_2O on Rh(111) adsorbed at 20 K as a function of coverage (the high coverage region from 0.96 to 16.69 BL). All the spectra were measured at 20 K with 4 cm^{-1} resolution and 500 scans.

3. Results and Discussion

3.1. Coverage Dependence of Water Molecules on Rh-(111) at 20 K. A series of IRAS spectra of D_2O adsorbed on Rh(111) at 20 K were measured as a function of water coverage (Figure 1a and Figure 1b). All the spectra were measured at 20 K. Figures 1a and 1b show the IRAS spectra in the low coverage region (0.02 to 0.67 BL) and in the high coverage region (0.96 to 16.69 BL), respectively. In the low coverage region (Figure 1a), each spectrum was obtained by the average of five individual spectra in order to achieve a good signal-to-noise ratio sufficient to distinguish the weak absorption of water molecules. All IRAS measurements in Figure 1a were performed in the following manner. First, a background reference spectrum was recorded on a clean Rh(111) surface, followed by the deposition of gaseous water molecules. A sample spectrum was measured on each adsorbate surface and divided by the background reference spectrum to obtain an absorption spectrum. Then, a new clean Rh(111) surface was obtained by flashing the sample to 300 K. The above-described cycle was repeated. The use of the pulse gas dosing system made each exposure highly reproducible and allowed the above averaging procedure. In the high coverage region (Figure 1b), in contrast, each absorption spectrum was obtained by dividing the same reference spectrum into each sample spectrum.

At a low coverage of 0.02 BL, only one sharp peak at 1161 cm^{-1} is observed in the DOD bending (δ_{DOD}) region. In the OD stretching (ν_{OD}) region, no peak is detected under the present experimental condition.

At 0.03 BL, the peak at 1161 cm^{-1} increases in intensity and a new peak appears at 1173 cm^{-1}. No peaks are observed in the ν_{OD} region.

At 0.13 BL, in the δ_{DOD} region the peak at 1161 cm^{-1} remains unchanged in intensity and shows a small red shift to 1159 cm^{-1}, whereas the peak at 1173 cm^{-1} develops in intensity. At the same time, a broad peak at 2570 cm^{-1} appears in the ν_{OD} region.

At 0.16 BL, the peak at 1173 cm^{-1} continues to develop in intensity in contrast to the decrease in intensity of the peak at 1159 cm^{-1}. A new band at 1188 cm^{-1} starts to appear. In the ν_{OD} region, the band around 2570 cm^{-1} increases in intensity and a lower wavenumber shoulder at 2560 cm^{-1} starts to appear as a new absorption band. In addition, two peaks are newly observed at 2700 and 2690 cm^{-1} in the ν_{OD} region. Broad absorption peaks are observed at 2630 and 2450 cm^{-1}.

At 0.30 BL, the bands at 1173 and 1188 cm^{-1} continue to develop in intensity, whereas the peak at 1159 cm^{-1} decreases further in intensity. In the ν_{OD} region, all the bands at 2700, 2690, 2630, 2560, and 2450 cm^{-1} develop in intensity. A new band appears around 2200 cm^{-1}.

At 0.46 BL, the peak at 1159 cm^{-1} almost disappears and the intensity of the peak at 1173 cm^{-1} remains unchanged, whereas the shoulder peak at 1188 cm^{-1} continues to develop in intensity. In the ν_{OD} region, all the bands at 2700, 2690, 2630, 2560, 2450, and 2200 cm^{-1} are increased in intensity.

At 0.67 BL, the peak at 1173 cm^{-1} decreases in intensity and the band at 1188 cm^{-1} increases in intensity. A broad absorption feature around 1210 cm^{-1} appears. In the ν_{OD} region, new peaks are observed at 2750 and 2731 cm^{-1} and the bands around 2560 and 2450 cm^{-1} develop in intensity, while the features at 2700, 2690, and 2630 cm^{-1} decrease in intensity. The broad feature is observed around 2200 cm^{-1}.

At 0.96 BL in Figure 1b, the peak at 1200 cm^{-1} appears in the δ_{DOD} region and the absorption around 1220 cm^{-1} enhances the intensity. In the ν_{OD} region, the features around 2550 and 2450 cm^{-1} show one broad absorption band with a broad shoulder around 2200 cm^{-1}, while the bands at 2700, 2690, and 2630 cm^{-1} diminish in intensity. The peaks at 2750 and 2731 cm^{-1} show an increase in intensity.

At 1.19 and 1.81 BL, in the δ_{DOD} region the peak at 1200 cm^{-1} and the shoulder feature around 1220 cm^{-1} continue to increase in intensity. In the ν_{OD} region, the broad band around 2550 cm^{-1} develops in intensity and the peaks at 2750 and 2731 cm^{-1} keep increasing in intensity. The shoulder peak around 2200 cm^{-1} becomes barely visible above 1.81 BL.

At coverages larger than 2.91 BL, the δ_{DOD} mode shows a blue shift and the shoulder peak at 1230 cm^{-1} starts to be observed. In the ν_{OD} region, the broad band around 2550 cm^{-1} continues to develop in intensity and the peaks at 2750 and 2731 cm^{-1} show a constant intensity.

TABLE 1: Comparison and Assignment of Vibrational Wavenumbers of Water Clusters

cluster size n	$(H_2O)_n$	$(D_2O)_n$	this study	assignments
1	3733[a]	2772[a]		ν_{as}
	3638[a]	2658[a]		ν_s
	1590[a]	1176[a]	1161	δ
2	3726[a]	2766[a]		acceptor-ν_{as}
	3709[a]	2746[a]	2700	donor-ν_{as}
	3634[a]	2655[a]		acceptor-ν_s
	3574[a]	2615[a]	2570	donor-ν_s
	1611[a]	1189[a]	1173	donor-δ
	1593[a]	1178[a]		acceptor-δ
3	3707[b]	2738[b]	2690	free OD
			2630	
	3516[b]	2579[b]	2560	bonded OD
			2450	
	1632, 1620[a]	1196[a]		δ
	1602[a]	1183[a]		δ
4	3714[d]	2735[e]	2690	free OD
			2630	
	3379[c]	2488[e]	2560	bonded OD
			2450	
			1188	δ
5	3714[d]	2735[e]	2690	free OD
			2630	
	3338[c]	2458[e]	2560	bonded OD
			2450	
			1188	δ
6			2690	free OD
			2630	
	3319[c]	2444[e]	2560	bonded OD
			2450	
			1188	δ

[a] Bentwood et al.[37] [b] Engdahl et al.[38] [c] Fajardo et al.[39] [d] Huisken et al.[40] [e] The stretching frequencies in $(D_2O)_n$ ($n = 4, 5, 6$) are estimated from those of $(H_2O)_n$ reported by other researchers [refs 37−40]. The vibrational conversion factor $(H_2O)_n/(D_2O)_n$ of 1.358 is derived from the empirical value obtained by averaging the ratios of OH stretching frequencies to OD stretching frequencies for water clusters ($n = 1-3$). This value is consistent with the reported isotope energy ratios.[44,66]

3.2. Assignment of the Adsorbed Water Species. The vibrational peaks observed in Figures 1a and 1b are assigned as compared with the previously reported vibrational frequencies for water clusters and also by taking into consideration the development of observed peaks as described in Section 3.1. Table 1 summarizes the comparison of the present results with the results from matrix isolation measurements[37−39] and infrared molecular depletion and fragment spectroscopy.[40]

At the very early stage of water adsorption on Rh(111), the peak at 1161 cm^{-1} is assigned to the δ_{DOD} mode for adsorbed water monomers (Figure 2a). A water monomer is thought to adsorb preferentially at an atop site on several closed-packed metal surfaces via its oxygen lone pair.[1,41] The molecular plane of water is nearly parallel to the surface according to theoretical DFT calculations.[42] An isolated water molecule in the gas phase has three normal modes of vibration: symmetric stretching (ν_s), asymmetric stretching (ν_{as}), and bending (δ_{DOD}) modes. For a water molecule adsorbed on metal surfaces with C_{2v} symmetry, however, the ν_{as} mode should not be observed by the surface selection rule of IRAS. In the present case, only the δ_{DOD} mode at 1161 cm^{-1} is observed for adsorbed water monomers since the absorption intensity of the ν_s mode is very small. The weak intensity of the ν_s mode is consistent with the fact that a water monomer adsorbs on the Rh(111) surface with its molecular plane nearly parallel to the surface. The strong intensity of the δ_{DOD} mode for adsorbed water monomers could be explained by a large dynamic dipole moment, which is induced by a coupling of the δ_{DOD} vibration of the adsorbed water molecule with the metal electronic state. Vibrational features of water

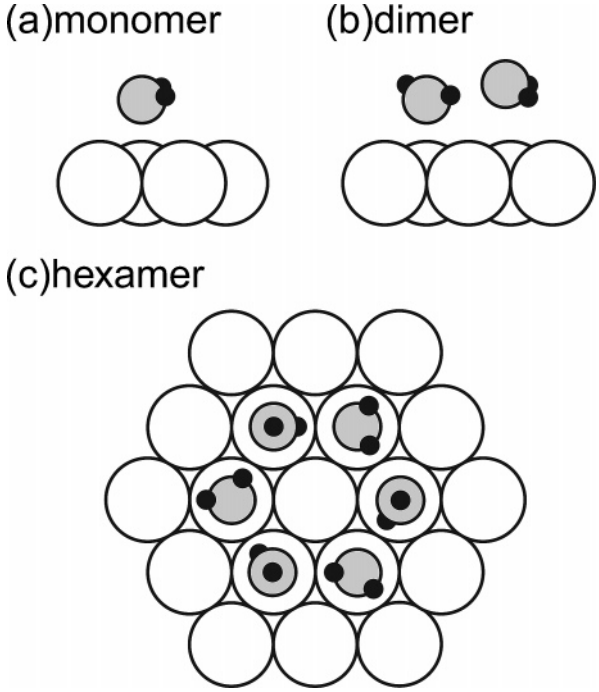

Figure 2. Schematic structural model for water clusters on Rh(111): (a) monomer, (b) dimer, and (c) hexamer species.

monomer species have been observed at 2531 and 1157 cm^{-1} on Ru(001)[26,27] and at 2474 and 1161 cm^{-1} on Ni(111).[28]

When the water coverage increases (0.03 and 0.13 BL), the 1173 and 2570 cm^{-1} peaks appear at the same time. Thus, these two vibrational peaks originate from the same water species. This water species is derived from larger water clusters than monomers, because its bending mode shows a blue shift from 1161 to 1173 cm^{-1}. Furthermore, the blue shift of 12 cm^{-1} is in agreement with the shift of 13 cm^{-1} in matrix isolation experiments from a monomer (1176 cm^{-1}) to a dimer (1189 cm^{-1}) (see Table 1). Therefore, the peaks at 1173 and 2570 cm^{-1} are assigned to the δ_{DOD} and ν_s mode of the proton-donor water molecule for adsorbed dimer species (Figure 2b), respectively.

When the water coverage is further increased to 0.16 BL, new bands appear at 1188 cm^{-1} in the δ_{DOD} region and at 2700, 2690, 2630, 2560, and 2450 cm^{-1} in the ν_{OD} region. The decrease in intensity of the δ_{DOD} mode for monomers at 1159 cm^{-1} indicates that water monomers aggregate to form larger clusters as the coverage of water increases.

The peaks at 2700, 2690, and 2630 cm^{-1} are ascribed to free OD of water clusters, while the peaks at 2560 and 2450 cm^{-1} are derived from hydrogen-bonded (H-bonded) OD of water clusters. Based on the comparison with the vibrational frequencies of water clusters in Table 1, the peak at 2700 cm^{-1} is assignable to ν_{as} of the proton-donor water molecule in the dimer; the peaks at 2690 and 2630 cm^{-1} can be assigned to the free OD mode for clusters larger than a trimer ($n = 3$). A similar assignment was reported for the peaks at 2707 and 2690 cm^{-1} on Ru(001): the 2707 cm^{-1} peak was assigned to ν_{as} of the proton-donor water molecule for dimers, whereas the 2690 cm^{-1} peak was assigned to the free OD mode of tetramers.[26] As shown in Table 1, the frequencies of free OD stretching vibrations show little change upon the cluster size increase from a trimer ($n = 3$) to a pentamer ($n = 5$), while the positions of the H-bonded OD stretching modes depend much more sensitively on the cluster size. Thus, it is difficult to assign the free OD modes at 2690 and 2630 cm^{-1} to the cluster of a specific

size. Although the bonded OD is sensitive to the cluster size, the bands at 2560 and 2450 cm^{-1} are too broad to be assigned to a specific sized cluster.

The band at 1188 cm^{-1} can be assigned to the δ_{DOD} mode of water clusters larger than tetramer ($n = 4$). This is because the blue shift (27 cm^{-1}) of this species from monomers cannot be explained by the peak shift (20 cm^{-1}) of a trimer in matrix isolation experiments (see Table 1). If we take into consideration that the 1188 cm^{-1} peak appears simultaneously with the 2690, 2630, 2560, and 2450 cm^{-1} peaks, all of these five peaks have the same origin and are attributed to water clusters larger than a tetramer ($n = 4$). However, we cannot exclude the existence of trimer species on the surface. Therefore, we conclude that the 2690, 2630, 2560, 2450, and 1188 cm^{-1} peaks are derived from large water clusters ($n = 3-6$) and different sized clusters may coexist on the surface. As an example of different sized clusters, a model structure of a hexamer ($n = 6$) is schematically shown in Figure 2c.

At coverages of 0.30 and 0.46 BL, large water clusters ($n = 3-6$) increase their coverages. The 2200 cm^{-1} peak can be assigned to a D_2O molecule with an OD bond pointing to the metal surface.[43] Such water molecules could exist at the edge of large clusters and/or 2D water islands. Such an extremely low-frequency band was reported for H_2O/Pt(100);[44] it was attributed to the O−H bond, which was H-bonded to the metal surface. Similar "softening" was observed for the CH stretching (ν_{CH}) modes of hydrocarbons adsorbed on metal surfaces, where they were also assigned to C−H bonds which were pointing toward the metal surface.[45,46]

When the water coverage further increases (0.67 and 0.96 BL), the small peaks at 2750 and 2731 cm^{-1} appear, which are derived from the ν_{OD} modes of "dangling OD" (free OD) groups with 2-coordinated and 3-coordinated surface D_2O molecules in bulk water ices, respectively.[47,48] The appearance of these peaks at 0.67 BL indicates that three-dimensional (3D) water islands start to be formed at this coverage. In addition, the free OD peaks at 2690 and 2630 cm^{-1} decrease in intensity, while the H-bonded OD peaks at 2560 and 2450 cm^{-1} and the δ_{DOD} mode at 1188 cm^{-1} continue to develop in intensity. As the 3D water islands are formed, the free OD peaks at 2690 and 2630 cm^{-1}, characteristic of large clusters and/or 2D water islands, diminish in intensity; instead, the free OD peaks at 2750 and 2731 cm^{-1}, characteristic of 3D water islands, increase. On the contrary, the H-bonded OD peaks at 2560 and 2450 cm^{-1} show an increase in intensity, because the H-bonded OD species in large clusters and/or 2D water islands may be in a similar H-bonding environment to the H-bonded OD species in 3D water islands.

At higher coverages from 1.19 to 16.69 BL, the δ_{DOD} mode shows a blue shift and the broad ν_{OD} band around 2550 cm^{-1} develops in intensity. At 16.69 BL, the broad peaks at ~2550, ~1630, ~1200, and ~650 cm^{-1} are observed (Figure 3). This spectrum is similar to that of amorphous ice that has been observed by other researchers.[49,50] Thus, it can be concluded that the bulk amorphous water ice layer is formed. The strong and broad peak around 2550 cm^{-1} is attributed to the OD stretching mode (ν_{OD}) with H-bonding in bulk and some contribution from overtone of the DOD bending mode (δ_{DOD}). The 1200 cm^{-1} peak is mainly due to the δ_{DOD} mode. The 650 cm^{-1} peak is ascribed to the hindered rotation mode (ν_L). The broad peak around 1630 cm^{-1} is ascribed to the association band of $3\nu_L$ and $\delta_{DOD} + \nu_L$.[51] Small but sharp peaks at 2750 and 2731 cm^{-1} are derived from OD stretching modes of "dangling OD" groups with 2-coordinated and 3-coordinated surface D_2O molecules, respectively.[47,48]

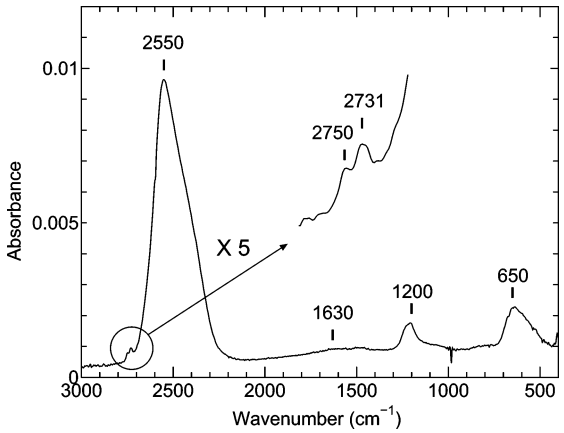

Figure 3. IRAS spectrum of D_2O (16.69 BL) on Rh(111) adsorbed at 20 K. The spectrum was measured at 20 K with 4 cm^{-1} resolution and 500 scans. The region from 2800 to 2650 cm^{-1} is magnified for clarity.

The coverage dependence of water molecules on the Rh(111) surface at 20 K is summarized as follows. At the initial stage of adsorption, water molecules exist as monomers. With increasing water coverage, monomers aggregate to form dimers and larger clusters ($n = 3-6$). Further exposure of water molecules leads to the formation of 2D water islands and then to 3D water islands, and finally to a bulk amorphous ice layer.

3.3. Temperature Dependence of Water Molecules on Rh-(111) ($\theta = 0.13$ BL). Figure 4 shows the IRAS spectra for 0.13 BL of water (D_2O) clusters on Rh(111) as a function of temperature. In Figure 4, each spectrum was obtained by the average of five individual spectra, as described for Figure 1a. To measure each spectrum, the 0.13 BL water (D_2O) molecules adsorbed at 20 K were heated to the indicated temperatures and then IRAS spectra were measured after the substrate was cooled to 20 K.

At 20 K (see Figure 4a), water molecules at a small coverage of 0.13 BL show a broad peak at 2570 cm^{-1} in the ν_{OD} region, and sharp peaks at 1159 and 1173 cm^{-1} in the δ_{DOD} region, as shown in Figure 1a. The peak at 1159 cm^{-1} is attributed to monomer species, while the peaks at 1173 and 2570 cm^{-1} are ascribed to dimers (see Section 3.2). Thus, both monomers and dimers coexist on Rh(111) at 20 K.

After heating to 80 K, in the ν_{OD} region new peaks are observed at 2690, 2650, and 2450 cm^{-1} and the band at 2570 cm^{-1} is broadened and shifted to 2550 cm^{-1}. In the δ_{DOD} region, two peaks at 1159 and 1173 cm^{-1} decrease in intensity and a new peak appears at 1188 cm^{-1}.

After heating to 140 K, the peaks at 2690 and 2450 cm^{-1} show an increase in intensity, whereas the peaks at 2650 and 2550 cm^{-1} decrease in intensity. In the δ_{DOD} region, two peaks at 1159 and 1173 cm^{-1} continue to decrease in intensity; but the intensity around 1188 cm^{-1} continues to develop.

After heating to 160 K, all four ν_{OD} bands observed at 140 K lose their intensity due to the desorption of water molecules on Rh(111). The bands at 2650 and 2550 cm^{-1} almost disappear in intensity. In the δ_{DOD} region, the intensity around 1210 cm^{-1} develops further. After heating to 200 K, all the absorption bands disappear.

As described above, upon heating, four ν_{OD} peaks are observed at 2690, 2650, 2550, and 2450 cm^{-1} and new δ_{DOD} peaks appear at 1188 cm^{-1} and higher wavenumbers. These bands are assigned to larger water clusters ($n = 3-6$) and/or

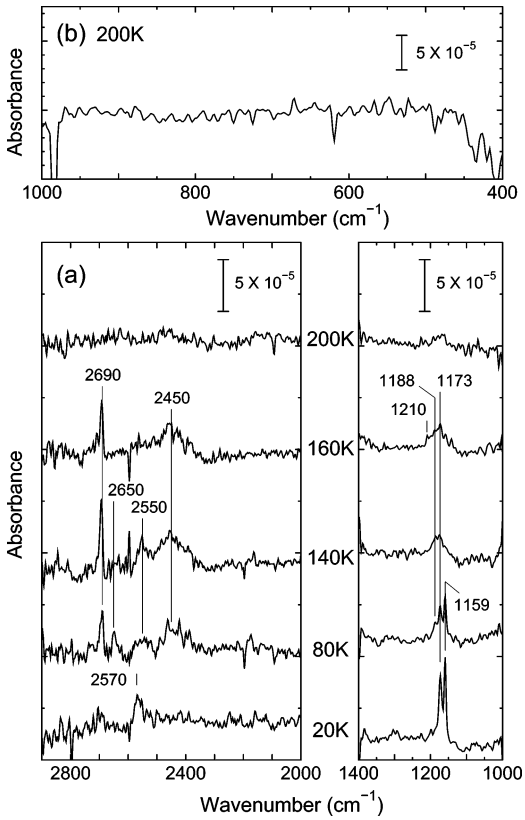

Figure 4. (a) IRAS spectra of D_2O (0.13 BL) on Rh(111) adsorbed at 20 K, followed by heating to 80, 140, 160, and 200 K. (b) IRAS spectrum from 1000 to 400 cm^{-1} for D_2O (0.13 BL) on Rh(111) after heating to 200 K. A sharp depression at ~980 cm^{-1} is due to instrumental noise. All the spectra were measured at 20 K with 4 cm^{-1} resolution and 1000 scans. Each spectrum presented here is the average of five individual spectra.

2D water islands as explained in Section 3.2. At the same time, the monomer and dimer peaks show a decrease in intensity. Therefore, upon heating, the monomer and dimer species migrate on the Rh surface by thermal excitation and aggregate to form larger clusters and/or 2D water islands.

After heating to 200 K, there are no absorption bands derived from molecular waters. In addition, no absorption bands derived from the dissociated water species (OD, O, and D) are observed (see Figure 4b); the vibrational peaks derived from Rh−D were observed at 480−536 cm^{-1} (60−67 meV) and ~784 cm^{-1} (~98 meV) as a function of the D coverage.[52] The Rh−O vibrational mode was observed at 530 cm^{-1}.[53] A hydroxyl species is not stable on Rh(111) and has never been isolated experimentally; on the Rh(111) surface, hydroxyls form a complex with adsorbed water molecules, $OH\cdot(H_2O)_x$ with $x = 0.5-1.5$.[31] The absorption peak of this complex was observed at 770 cm^{-1}.[31] Therefore, we conclude that a water molecule does not dissociate on the Rh(111) surface and desorbs as a water molecule by heating to 200 K.

Here it should be emphasized that four ν_{OD} peaks show a different temperature dependence upon heating: the peaks at 2690 and 2450 cm^{-1} increase in intensity, while the peaks at 2650 and 2550 cm^{-1} decrease in intensity. To interpret this temperature dependence of four ν_{OD} peaks, we propose the following scenario for water aggregation on Rh(111) upon heating. Heating the surface allows greater mobility of monomer and dimer species, and larger water clusters and/or 2D water islands are formed. The most stable water clusters at higher temperatures would be cyclic hexamers for the following reasons. First, recent STM observations demonstrate the existence of cyclic hexamers on various metal surfaces including Cu(111)[14,15] and Pd(111)[18,19] even at low temperatures. At high temperatures above 70 K, 2D islands and 2D water layers consisting of cyclic hexamers are observed on Ag,[11−13] Pt,[16,17] and Pd[19] surfaces. Second, the building block of the "bilayer" ice on hexagonal closed-packed metal surfaces is a cyclic hexamer.[1,2] The "bilayer" ice is a thermodynamically stable water adlayer because it is usually grown at high temperatures just below the desorption temperature. Thus, cyclic hexamers are the most stable form of water molecules on hexagonal metal surfaces. Third, recent DFT calculations show that cyclic hexamers are the most stable water clusters on metal surfaces.[54,55]

On the basis of the above discussion, we conclude that the observed four ν_{OD} peaks are mainly derived from cyclic hexamer species. After the mild anneal to 80 K, small water clusters ($n = 3-5$) may coexist on the surface, but the most dominant water species would be the cyclic hexamer. Further heating results in the aggregation of cyclic hexamers into larger 2D water islands. As the size of 2D islands increases with increasing temperature, the number of water molecules inside 2D islands increases, while that of water molecules at the edge of 2D islands decreases. *Therefore, we conclude that the peaks at 2690 and 2450 cm^{-1} are derived from water molecules inside 2D islands, whereas the peaks at 2650 and 2550 cm^{-1} originate from water molecules at the edge of 2D islands.*

The assignment of each ν_{OD} peak is conducted in the following way. The traditional "bilayer" model[3] is assumed as the model of 2D water islands. In the "bilayer" model, all ν_{OD} modes can be classified into four groups as is schematically shown in Figure 5: free OD and H-bonded OD of water molecules inside 2D islands and free OD and H-bonded OD of water molecules at the edge of 2D islands. Taking into account the above discussion and the fact that the ν_{OD} mode shows a red shift upon hydrogen bonding, four ν_{OD} peaks are assigned as follows: the peaks at 2690 and 2450 cm^{-1} are attributed to free OD and H-bonded OD of water molecules inside 2D islands, respectively; the peaks at 2650 and 2550 cm^{-1} are attributed to free OD and H-bonded OD of water molecules at the edge of 2D islands, respectively.

3.4. Comparison with Clustering Behaviors on Other Metal Surfaces. In this section, the present results on Rh(111) are compared with the previous results on Ni(111),[28] Pt(111),[25] and Ru(001)[26,27] reported by Nakamura et al. Figure 6a−c (taken from Figure 4 in ref 28) shows the IRAS spectra for D_2O adsorbed on Ni(111), Pt(111), and Ru(001) at 20 K, respectively. The water coverage is about 0.5 BL. Figure 6d shows the IRAS spectrum for D_2O (0.46 BL) adsorbed on Rh(111) at 20 K, as is also shown in Figure 1a.

On all metal surfaces, there exist four peaks at similar wavenumbers (~2690, ~2650, ~2550, and ~2450 cm^{-1}) in the ν_{OD} region, which originate mainly from cyclic hexamer species as discussed in Section 3.3. This indicates that the predominant water cluster species is the cyclic hexamer on these hexagonal metal surfaces. Another important point to note here is that on Ni(111) and Pt(111) the 2690 and 2450 cm^{-1} peaks are much stronger in intensity than the 2650 and 2550 cm^{-1} peaks; on Ru(001) and Rh(111) the intensity of the 2690 and 2450 cm^{-1} peaks is less intense than that on Ni(111) and Pt(111) and is comparable with the 2650 and 2550 cm^{-1} peaks. Since the 2690 and 2450 cm^{-1} peaks are ascribed to water molecules inside 2D islands and the 2650 and 2550 cm^{-1} peaks to water molecules at the edge of 2D islands (see Section 3.3),

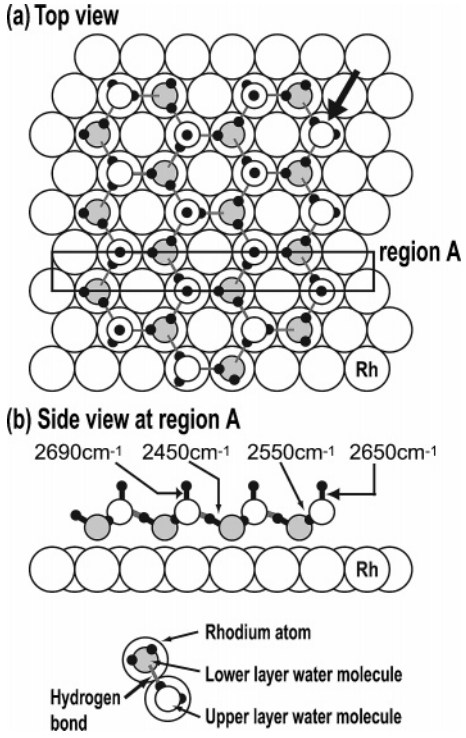

Figure 5. Schematic structural model for a two-dimensional (2D) water island: (a) top view and (b) side view of region A. Water molecules in the 2D island are arranged in the "bilayer" structure. All OD stretching modes in this structure can be divided into four groups: free OD and H-bonded OD of water molecules inside the 2D island and free OD and H-bonded OD of water molecules at the edge of the 2D island. The peak positions observed in the experiment (Figure 4a), corresponding to each vibrational mode, are shown. Note that some water molecules at the edge of the 2D island may have the OD bond pointing to the metal surface (see the arrow in the figure).

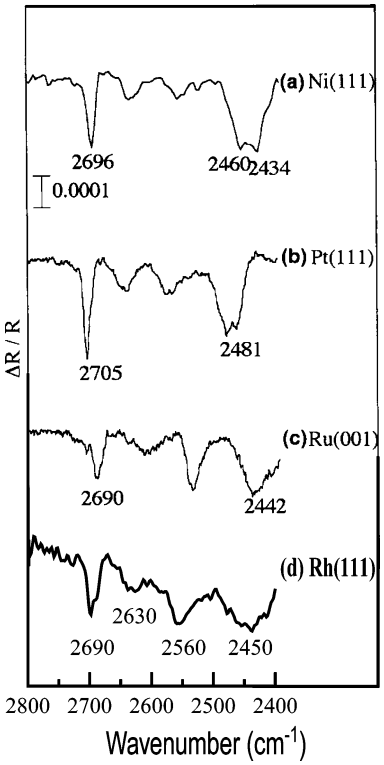

Figure 6. IRAS spectra of water (D_2O) clusters on Ni(111) (a), Pt-(111) (b), Ru(001) (c), and Rh(111) (d) at 20 K. The water coverage is (a) 0.50, (b) 0.51, (c) 0.53, and (d) 0.46 BL. All the spectra are shown with a vertical axis of reflectivity. Spectra a−c are taken from ref 28 with permission.

we conclude that smaller sized 2D islands, where the number of water molecules at the edge of islands is larger, are formed on Ru(001) and Rh(111) surfaces than on Ni(111) and Pt(111) surfaces.

As for the desorption temperature in TPD spectra for the first layer water molecules, higher desorption peaks are observed on Ru(001) (220 K[3,56]) and Rh(111) (180−190 K[30,31]) than on Ni(111) (∼170 K[57,58]) and Pt(111) (∼170 K[59,60]). This indicates that the desorption barriers on Ru(001) and Rh(111) are larger than those on Ni(111) and Pt(111). In general, the diffusion barriers are closely related to the desorption barriers.[61,62] Thus, the diffusion barriers on Ru(001) and Rh(111) would be larger than those on Ni(111) and Pt(111). In consequence, water molecules do not migrate very much on Ru(001) and Rh(111) surfaces, which leads to the formation of small 2D islands. On the contrary, on Ni(111) and Pt(111) surfaces which have smaller diffusion barriers than Ru(001) and Rh(111), water molecules can migrate on the surfaces easily and form large 2D islands. This adsorption model qualitatively explains the IRAS spectra well.

It should be noted that the thermal migration is suppressed at a low temperature of 20 K. Thus, the clustering of water molecules on low-temperature metal surfaces is mainly governed by the "transient migration" of an adsorbing molecule. When a gaseous molecule adsorbs on the surface, the adsorption energy has to be dissipated. This leads to not only the excitation of various motions of the molecule on the surface (lateral translations, internal vibrations, and rotations), but also electron−hole pair and phonon excitations of the substrate.[63−65] Accordingly, the "transient migration" stands for the lateral motion of an incoming molecule to the surface during the dissipation of the adsorption energy.[62] The "transient migration" should largely depend on the shape of the potential energy surface (PES). Since the diffusion barrier, which represents the corrugation of PES across the surface, is relatively large for the present D_2O/Rh(111) system, the transient migration of an adsorbing water molecule is relatively limited. This results in the formation of smaller 2D water islands on Rh(111).

4. Conclusion

We investigated the clustering behavior and ice layer formation of water (D_2O) molecules on Rh(111) at 20 K using IRAS.

At a very low coverage, water molecules exist as monomers on Rh(111). With increasing water coverage, monomers aggregate to form dimers, larger clusters ($n = 3-6$), and 2D islands. Further exposure of water molecules leads to the formation of 3D water islands and finally to a bulk amorphous ice layer.

Upon heating, the monomer and dimer species thermally migrate on the Rh surface and aggregate to form larger clusters and 2D islands. By heating above 160 K, water molecules start to desorb from the Rh(111) surface without dissociation. Four ν_{OD} peaks (at 2690, 2650, 2550, and 2450 cm^{-1}), characteristic of 2D islands, show a different temperature dependence upon heating: the peaks at 2690 and 2450 cm^{-1} increase in intensity, while the peaks at 2650 and 2550 cm^{-1} decrease in intensity. Based on the model that the size of 2D islands increases with the temperature rise, these four ν_{OD} peaks can be assigned as follows: the peaks at 2690 and 2450 cm^{-1} are attributed to free OD and H-bonded OD of water molecules inside 2D islands, respectively; the peaks at 2650 and 2550 cm^{-1} are

attributed to free OD and H-bonded OD of water molecules at the edge of 2D islands, respectively.

From the comparison with the previous vibrational spectra for water clusters on other metal surfaces, we found that the number of water molecules at the edge of 2D islands is comparable with that of water molecules inside 2D islands on the Rh(111) surface at 20 K. This indicates that the size of 2D islands on Rh(111) is small. The strong water−substrate interaction on the Rh(111) surface makes the adsorbed water molecules experience a comparatively large diffusion barrier. Thus, the transient migration of water molecules is relatively limited on Rh(111) at 20 K; this results in the formation of smaller 2D islands on Rh(111). The present vibrational study clearly shows how the underlying substrate properties influence the clustering behavior of water molecules on low-temperature metal surfaces.

Acknowledgment. Financial support was provided in part by the Grant-in-Aid for Scientific Research on Priority Areas "Surface Chemistry of Condensed Molecules" from the Ministry of Education, Culture, Sports, Science and Technology (MEXT) of Japan. One of the authors (S.Y.) is supported by the program "The 21st century COE program for Frontiers in Fundamental Chemistry" at the University of Tokyo.

References and Notes

(1) Thiel, P. A.; Madey, T. E. *Surf. Sci. Rep.* **1987**, *7*, 211.
(2) Henderson, M. A. *Surf. Sci. Rep.* **2002**, *46*, 1.
(3) Doering, D. L.; Madey, T. E. *Surf. Sci.* **1982**, *123*, 305.
(4) Williams, E. D.; Doering, D. L. *J. Vac. Sci. Technol.* **1983**, *A1*, 1188.
(5) Held, G.; Menzel, D. *Surf. Sci.* **1994**, *316*, 92.
(6) Ogasawara, H.; Brena, B.; Nordlund, D.; Nyberg, M.; Pelmenschikov, A.; Pettersson, L. G. M.; Nilsson, A. *Phys. Rev. Lett.* **2002**, *89*, 276102.
(7) Feibelman, P. J. *Science* **2002**, *295*, 99.
(8) Michaelides, A.; Alavi, A.; King, D. A. *J. Am. Chem. Soc.* **2003**, *125*, 2746.
(9) Denzler, D. N.; Hess, Ch.; Dudek, R.; Wagner, S.; Frischkorn, Ch.; Wolf, M.; Ertl, G. *Chem. Phys. Lett.* **2003**, *376*, 618.
(10) Ikemiya, N.; Gewirth, A. A. *J. Am. Chem. Soc.* **1997**, *119*, 9919.
(11) Morgenstern, K.; Nieminen, J. *Phys. Rev. Lett.* **2002**, *88*, 066102.
(12) Morgenstern, K. *Surf. Sci.* **2002**, *504*, 293.
(13) Morgenstern, K.; Nieminen, J. *J. Chem. Phys.* **2004**, *120*, 10786.
(14) Morgenstern, K.; Rieder, K.-H. *J. Chem. Phys.* **2002**, *116*, 5746.
(15) Morgenstern, K.; Rieder, K.-H. *Chem. Phys. Lett.* **2002**, *358*, 250.
(16) Morgenstern, M.; Michely, T.; Comsa, G. *Phys. Rev. Lett.* **1996**, *77*, 703.
(17) Morgenstern, M.; Müller, J.; Michely, T.; Comsa, G. *Z. Phys. Chem.* (*Munich*) **1997**, *198*, 43.
(18) Mitsui, T.; Rose, M. K.; Fomin, E.; Ogletree, D. F.; Salmeron, M. *Science* **2002**, *297*, 1850.
(19) Cerdá, J.; Michaelides, A.; Bocquet, M.-L.; Feibelman, P. J.; Mitsui, T.; Rose, M.; Fomin, E.; Salmeron, M. *Phys. Rev. Lett.* **2004**, *93*, 116101.
(20) Andersson, S.; Nyberg, C.; Tengstål, C. G. *Chem. Phys. Lett.* **1984**, *104*, 305.
(21) Jacobi, K.; Bertolo, M.; Geng, P.; Hansen, W.; Schreiner, J.; Astaldi, C. *Surf. Sci.* **1991**, *245*, 72.
(22) Jacobi, K.; Bedürftig, K.; Wang, Y.; Ertl, G. *Surf. Sci.* **2001**, *472*, 9.
(23) Ogasawara, H.; Yoshinobu, J.; Kawai, M. *Chem. Phys. Lett.* **1994**, *231*, 188.
(24) Ogasawara, H.; Yoshinobu, J.; Kawai, M. *J. Chem. Phys.* **1999**, *111*, 7003.
(25) Nakamura, M.; Shingaya, Y.; Ito, M. *Chem. Phys. Lett.* **1999**, *309*, 123.
(26) Nakamura, M.; Ito, M. *Chem. Phys. Lett.* **2000**, *325*, 293.
(27) Nakamura, M.; Ito, M. *Chem. Phys. Lett.* **2001**, *335*, 170.
(28) Nakamura, M.; Ito, M. *Chem. Phys. Lett.* **2004**, *384*, 256.
(29) Glebov, A. L.; Graham, A. P.; Menzel, A. *Surf. Sci.* **1999**, *427*−*428*, 22.
(30) Zinck, J. J.; Weinberg, W. H. *J. Vac. Sci. Technol.* **1980**, *17*, 188.
(31) Wagner, F. T.; Moylan, T. E. *Surf. Sci.* **1987**, *191*, 121.
(32) Röttger, K.; Endriss, A.; Ihringer, J.; Doyle, S.; Kuhs, W. F. *Acta Crystallogr.* **1994**, *B50*, 644.
(33) Gibson, K. D.; Viste, M.; Sibener, S. J. *J. Chem. Phys.* **2000**, *112*, 9582.
(34) Linke, R.; Curulla, D.; Hopstaken, M. J. P.; Niemantsverdriet, J. W. *J. Chem. Phys.* **2001**, *115*, 8209.
(35) Feulner, P.; Menzel, D. *J. Vac. Sci. Technol.* **1980**, *17*, 662.
(36) Yates, J. T., Jr. *Experimental Innovations in Surface Science*; Springer-Verlag: New York, 1998.
(37) Bentwood, R. M.; Barnes, A. J.; Orville-Thomas, W. J. *J. Mol. Spectrosc.* **1980**, *84*, 391.
(38) Engdahl, A.; Nelander, B. *J. Chem. Phys.* **1987**, *86*, 4831.
(39) Fajardo, M. E.; Tam, S. *J. Chem. Phys.* **2001**, *115*, 6807.
(40) Huisken, F.; Kaloudis, M.; Kulcke, A. *J. Chem. Phys.* **1996**, *104*, 17.
(41) Flores, F.; Gabbay, I.; March, N. H. *Surf. Sci.* **1981**, *107*, 127.
(42) Michaelides, A.; Ranea, V. A.; de Andres, P. L.; King, D. A. *Phys. Rev. Lett.* **2003**, *90*, 216102.
(43) Thiel, P. A.; DePaola, R. A.; Hoffmann, F. M. *J. Chem. Phys.* **1984**, *80*, 5326.
(44) Ibach, H.; Lehwald, S. *Surf. Sci.* **1980**, *91*, 187.
(45) Demuth, J. E.; Ibach, H.; Lehwald, S. *Phys. Rev. Lett.* **1978**, *40*, 1044.
(46) Yamamoto, M.; Sakurai, Y.; Hosoi, Y.; Ishii, H.; Kajikawa, K.; Ouchi, Y.; Seki, K. *J. Phys. Chem. B* **2000**, *104*, 7370.
(47) Rowland, B.; Devlin, J. P. *J. Chem. Phys.* **1991**, *94*, 812.
(48) Buch, V.; Devlin, J. P. *J. Chem. Phys.* **1991**, *94*, 4091.
(49) Whalley, E. *Can. J. Chem.* **1977**, *55*, 3429.
(50) Schaff, J. E.; Roberts, J. T. *J. Phys. Chem.* **1996**, *100*, 14151.
(51) Eisenberg, D.; Kauzmann, W. *The Structure and Properties of Water*; Oxford University Press: London, UK, 1969.
(52) Yanagita, H.; Fujioka, H.; Aruga, T.; Takagi, N.; Nishijima, M. *Surf. Sci.* **1999**, *441*, 507.
(53) Semancik, S.; Haller, G. L.; Yates, J. T., Jr. *Appl. Surf. Sci.* **1982**, *10*, 546.
(54) Meng, S.; Wang, E. G.; Gao, S. *J. Chem. Phys.* **2003**, *119*, 7617.
(55) Meng, S.; Wang, E. G.; Gao, S. *Phys. Rev. B* **2004**, *69*, 195404.
(56) Denzler, D. N.; Wagner, S.; Wolf, M.; Ertl, G. *Surf. Sci.* **2003**, *532*−*535*, 113.
(57) Pache, T.; Steinrück, H.-P.; Huber, W.; Menzel, D. *Surf. Sci.* **1989**, *224*, 195.
(58) Stulen, R. H.; Thiel, P. A. *Surf. Sci.* **1985**, *157*, 99.
(59) Haq, S.; Harnett, J.; Hodgson, A. *Surf. Sci.* **2002**, *505*, 171.
(60) Daschbach, J. L.; Peden, B. M.; Smith, R. S.; Kay, B. D. *J. Chem. Phys.* **2004**, *120*, 1516.
(61) Naumovets, A. G.; Vedula, Y. S. *Surf. Sci. Rep.* **1985**, *4*, 365.
(62) Barth, J. V. *Surf. Sci. Rep.* **2000**, *40*, 75.
(63) Billing, G. D. *Chem. Phys.* **1984**, *86*, 349.
(64) Tully, J. C. *Surf. Sci.* **1994**, *299*−*300*, 667.
(65) Rettner, C. T.; Ashford, M. N. R., Eds. *Dynamics of Gas*−*Surface Interactions*; Royal Society of Chemistry: Cambridge, UK, 1991.
(66) Yamada, T.; Okuyama, H.; Aruga, T.; Nishijima, M. *J. Phys. Chem. B* **2003**, *107*, 13962.